

# Nonlinear Optical Absorption of Carbon Nanostructures Synthesized by Laser Ablation of Highly Oriented Pyrolytic Graphite in Organic Solvents

Hajar Ghanbari<sup>a</sup>, Rasoul Sarraf-Mamoory<sup>a,\*</sup>, Jamshid Sabbaghzadeh<sup>b</sup>, Ali Chehrghani<sup>c</sup>, and Rasoul Malekfar<sup>d</sup>

<sup>a</sup>Materials Engineering Department, Tarbiat Modares University, Tehran, Iran.

<sup>b</sup>Center for Advanced Science and Technology, Islamic Azad University, Iran.

<sup>c</sup>Laser Materials Processing Lab. Iranian National Center for Laser Science and Technology, Tehran, Iran.

<sup>d</sup>Physics Department, Faculty of Basic Sciences, Tarbiat Modares University, Tehran, Iran.

\*Corresponding Author Email: [rsarrafm@modares.ac.ir](mailto:rsarrafm@modares.ac.ir)

**ABSTRACT**— In this study, Highly Oriented Pyrolytic Graphite was ablated in various polar and nonpolar solvents by Q-switched neodymium: yttrium-aluminum-garnet laser (wavelength=1064 nm, frequency=2 kHz, pulse duration=240 ns). Then, the products were examined using Scanning Electron Microscopy and UV-Vis spectroscopy. The images showed that different carbon structures such as cauliflower-like structures in benzene, spiral integrated forms in toluene, organic integrated networks in hexane, and nanoparticles in ethanol were formed. In n-methyl-2-pyrrolidone (NMP), sheets and bulk deformed structures were seen. Also, in Dimethylacetamide, particles in different stages of growth could be detected. The nonlinear optical absorption (NLA) behaviors of the products were investigated by exposing them to a 532 nm nanosecond laser using the Z-scan technique. The saturated NLA coefficient, obtained from structures of NMP and hexane-based synthesized samples, are  $1.1 \times 10^{-8}$  and  $-2.4 \times 10^{-8} \text{ cm W}^{-1}$ , respectively. The saturable absorption responses of these samples were switched to the reverse saturable absorption responses in the other synthesis mediums. The maximum nonlinear absorption coefficient of  $10.2 \times 10^{-8} \text{ cm W}^{-1}$  was measured for spiral integrated superstructures, produced in the toluene medium.

**KEYWORDS:** LP-PLA, Highly Oriented Pyrolytic Graphite, Nonlinear Optical Absorption, Organic Solvent, Nanostructures

## I. INTRODUCTION

Since the first laser ablation (LA) experiment in 1963 [1], a wide range of engineering and non-engineering materials have been ablated by laser. Due to the potential of thin layer preparation, nanocrystal growth, surface cleaning, tissue removing, etc. Laser ablation has been investigated from various points of view [2] by researchers all over the world. One of the most attractive LA application areas is nanostructure synthesis. Nanostructures which are synthesized via LA have unrivalled characteristics due to their exclusive path of nucleation & growth [3]-[7]. Two of the main materials used as targets in LA process are carbonaceous and graphitic structures which are studied according to their increasing tendency to the synthesis and application of carbon structures such as diamond, diamond-like carbons (DLCs), fullerenes, carbon nanotubes, and nanofibers [8]-[13].

Liquid-phase pulsed laser ablation (LP-PLA) has certain benefits compared to laser ablation in gas phase and vacuum, especially because of its ability to synthesize metastable structures which are not accessible in normal temperatures and pressures [14]. The physical mechanism of LP-PLA of solid target was previously studied by Berthe, *et al.* [15]. When a high-energy laser beam focuses on a target

surface, at the initial stage of the interaction, the particles are ablated with a large kinetic energy from the target surface and a dense plume is created in the solid–liquid interface. In addition, compared to air and vacuum, the covering effect of a liquid restricts the plasma plume and so, an adiabatical expansion occurs at a supersonic velocity. Therefore, a high pressure and temperature plasma are created and quenched in a short time, resulting in the growth of various nanostructures.

Recently, researchers have focused on the synthesis of metastable structures such as diamonds [8], [16], DLCs [17], and carbon nitrides [18] at room temperature. Most of the experiments have been carried out in water [17], [19], [20], although some other liquids have been used as mediums such as ammonia [21], 2propanol [22], benzene [23], [24], hexane, toluene [23], and ethanol [12]. These works have been studied in four areas of theory and simulation [25], [26], plasma plume in liquid environments [8], laser ablation mechanistic issues [25], [27], and final product investigation [3], [28]. In addition, the nonlinear optical (NLO) studies were mainly conducted on well-known carbon structures such as graphene, fullerene, carbon nanotubes, and on metal nanoparticles (NPs) decorated on these structures [29]-[34]. The NLO characteristics have been observed as a result of optical limiting in multi-walled carbon nanotubes (MWCNTs) [30] and single-walled carbon nanotubes (SWCNTs) [31]. Noble metal NPs supported on the surface of carbon nanotubes are also known to possess large nonlinear optical properties [30], [34]. However, NLO properties of more unknown carbon nanostructures with various morphologies have been paid less attention. One of these aspects is nonlinear optical absorption (NLA) which is measurable by open aperture Z-scan system. The sign of the NLA coefficient could be negative or positive depends on the inherent materials characteristics and experimental conditions (such as wavelength, intensity, and pulse duration of the laser used). Each of these behaviors originates from different physical

mechanisms. Negative NLA is known as saturation of absorption (SA). In this situation, the sample optical transmittance increases with increasing of the radiation intensity. In the case of a positive NLA, the propagated laser radiation was absorbed in the medium and material transmittance reduces with increasing of the optical intensity [35].

In this research, the solvent-dependency of carbon nanostructures' morphology synthesized in LP-PLA of highly oriented pyrolytic graphite (HOPG) has been investigated in order to explore the possibility of proposing new carbonaceous materials with improved NLA properties. For this purpose, the NLA behaviors of these nanostructures exposed to the 532 nm (10 ns pulse duration) laser radiation have been studied.

## II. EXPERIMENTS

### A. Synthesis Procedure

HOPG (NT-MDT, ZYB Quality) was placed at the bottom of a glass vessel filled with 2.5 cm<sup>3</sup> of distinct organic solvents including ethanol (Merck, >99.9%), toluene (Merck, >99.9%), n-hexane (Merck, >98%), benzene (Merck, >99.8%), dimethylacetamide (DMA) (Merck, >99.5%), and n-methyl-2-pyrrolidone (NMP) (Merck, >99.9%). The height of the solvent on top of the target is 1.5 mm and was later reduced during laser irradiation by different rates depending on the volatility of the solvent. To conduct the experiments, an acousto-optically Q-switched neodymium: yttrium-aluminum-garnet (Nd:YAG) laser (1064 nm) with 240 ns pulse duration, adjusted to operate at 2 kHz repetition rate, was employed. The energy density on the target, the so-called fluence, was about 13.65 J.cm<sup>-2</sup>.

Due to the toxic gas released through laser irradiation, a plexiglass box equipped with a suction pipe connected to a fan was designed to withdraw the gas. This box is fixed from top to the exit path of the laser beam and a suction tube joint with a fan is fixed on the other side of the box to conduct the gas out of the laboratory.

The arrangement of the laser apparatus, HOPG target in vessel and protective set are schematically shown in Fig. 1. The irradiation time in these experiments was 20 min and the focal spot size was 70  $\mu\text{m}$ . The laser ablation also was done at room temperature.

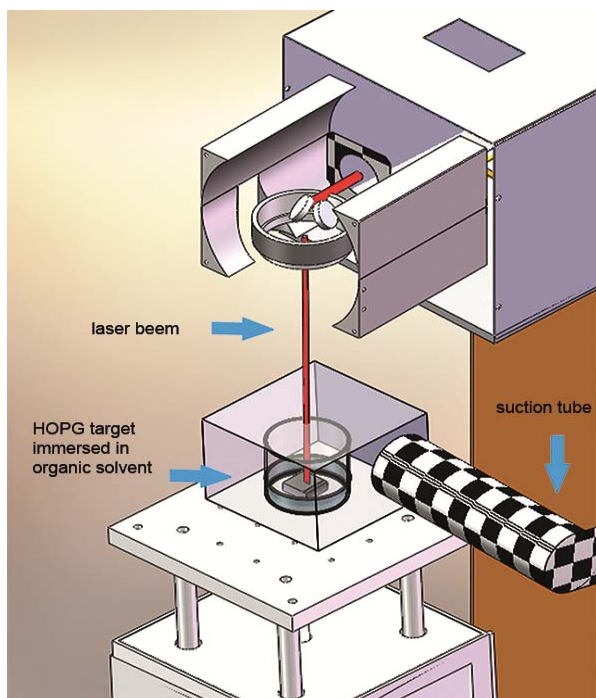


Fig. 1: Schematic of laser apparatus, protective box, and suction tube.

### B. Characterization

The as-synthesized samples were ultrasonicated for 20 min with an ultrasonic cleaner (Labbrethe 17, FR/TSCH, 140 W, 50 Hz). Scanning Electron Microscopy (SEM) samples, prepared by drop casting followed by Au coating, were investigated (Hitachi SE-4160 Field Emission Gun Scanning Electron Microscopy (FEG-SEM), Japan and LEO 1530 Gemini FEG-SEM, Cambridge, U.K.). Some of the applied solvents had relatively high UV cut-off edges. So, for UV-Vis spectroscopy, the liquid environment was replaced with ethanol using simple decantation without drying to avoid secondary agglomeration. The final colloidal solution was transferred into a 10 mm quartz cell and the UV-Vis absorption spectra were taken (Lambda 25 model, Perkin Elmer Inc.) in a 190–1100 nm scan range and 2 nm resolution.

### C. Z-scan set-up

The nonlinear optical properties of carbon nanostructures were investigated by applying Z-scan technique, which was developed by Bahae *et al.* [36]. This technique, due to its simplicity and high sensitivity, is a common method to measure optical nonlinear behavior of materials. In this technique, the self-focusing/defocusing response of the materials under laser irradiation determines the NLA and the refraction. For this purpose, a focused single Gaussian laser beam is exposed onto a nonlinear medium, as illustrated in Fig. 2.

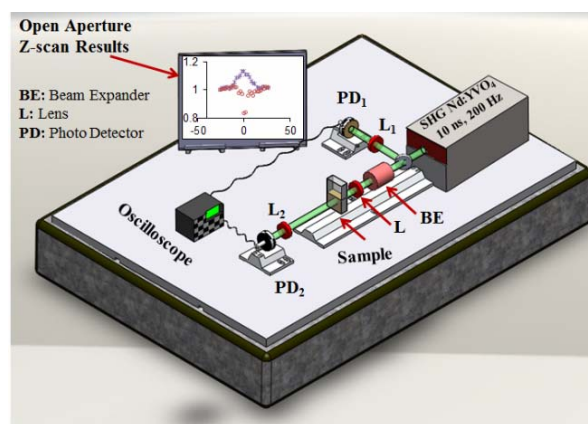


Fig. 2: Experimental setup of Z-scan technique

Sample transmittance with a finite aperture is measured in the far field as a function of the sample position (on z axis). The sample position is defined with respect to the focal plane of L lens in Fig. 2. To perform the Z-scan experiments, a Q-switched neodymium-doped yttrium orthovanadate laser from the EKSPLA Company (model NL640) was used. The light source was coupled with a second harmonic generation (SHG) unit which generates 532 nm laser pulses with 10 ns pulse duration. A lens with a focal length of 80 mm was used (L lens in Fig. 2) to focus the laser beam on a 70  $\mu\text{m}$  spot diameter, as determined with the knife-edge technique. The laser operates at 200 Hz pulse repetition rate and 0.03 mJ pulse energy. The maximum laser beam intensity at focal point is  $7.02 \times 10^7 \text{ W}\cdot\text{cm}^{-2}$  on the sample surface. The colloidal suspension of various carbon nanostructures was transferred to a 2 mm quartz cuvette, which was fixed on a translation stage

and moved over the 60 mm length through both sides of the focal region of the laser beam. The sample was moved 2 mm in each step and position-dependent transmission was measured in an oscilloscope by using photodiodes (PD2) for open aperture trace of the Z-scan setup. The detected signals were stored and compared with the main laser beam signals (PD1 in Fig. 2), which are used to calculate the NLA coefficients of these suspensions.

### III. RESULTS AND DISCUSSION

#### A. Structural characterization

Figure 3 shows the lamellar structure of ablating HOPG target. The typical ablated surface of the HOPG in these solvents is seen in the inset of Fig. 3. The typical deep crater, which is usually formed as a result of the laser beam collision with the target during the ablation process, is not seen in any of these experiments. The Scraping of the outer layer of the HOPG is the tangible effect observed on the targets after ablation which was seen in all the tested solvents.

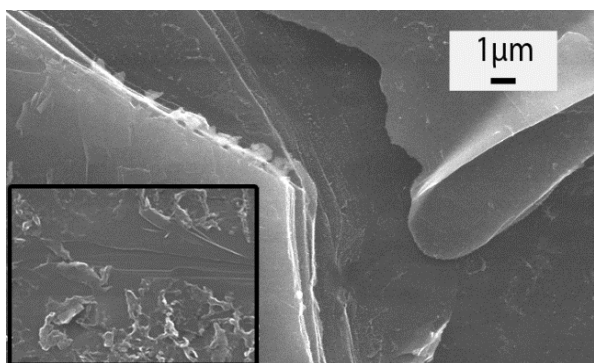


Fig. 3: SEM of HOPG lamellar structure. Inset: the scraping of the outer layer of HOPG after laser ablation

SEM images of synthesized structures in various solvents; two aromatic hydrocarbons (toluene and benzene), an alkane (n-hexane), an alcohol (ethanol), a cyclic amide (NMP), a polar organic solvent (DMA), and finally an alkane (hexane) are illustrated in Fig. 4. A

spiral integrated structure of more than ten micrometers in length was formed in the product of HOPG ablation in toluene (Fig. (4.a)). Its fine structure can be seen in Fig. (4.b-c). The chains twisting in different directions are observed in the 2D view of the product in medium magnification. More focused image in Fig. (4.c) reveals the 3D structure in different steps of growth. While some features are at their initial stages and just look like seeds (Section 1), the other Sections are in the intermediate steps of growth (horizontal growth in Section 2), and the last Sections are in the final stage of boosting (vertical growth in Section 3) which form spiral oriented nanowalls. Unlike the prepared samples in toluene, the individual ball-shape superstructures are seen in a benzene environment (Fig. (4.d)). Detailed features of this superstructure are shown in Figs. (4.e-f). A Cauliflower-like structure is the overall appearance of the product. Nanowalls of less than 1  $\mu\text{m}$  in thickness are the fine components of this superstructure. SEM images of the product prepared by the ablation of HOPG in ethanol are illustrated in Fig. (4.g-i) in which the cut-off slices, agglomerated, and individual nanoparticles of 10-50 nm are observed. As it can be seen, some of the agglomerated nanoparticles are joining to make 100 nm spherical particles (Fig. (4.h)), and some are forming shapeless agglomerates. In DMA, nanoparticles of different sizes, micrometer size cubic and spherical particles are observed (Fig. (4.g-l)). The spherical morphology of particles changes to cubic structures through growth. The addition of small particles to the cubes seems to be the cause of growing which is shown in Fig. (4.l) inset. Distinct structures are fabricated in n-hexane: non-agglomerated nano/micro size cubes (Fig. (4.m)), severely agglomerated nanoparticles (Fig. (4.n)), and somehow diffused and sintered particles (Fig. 4.o). In NMP, graphitic sheets with different lateral size and thickness are seen (Fig. (4.p)). More magnified images are shown in Fig. (4.q-r).

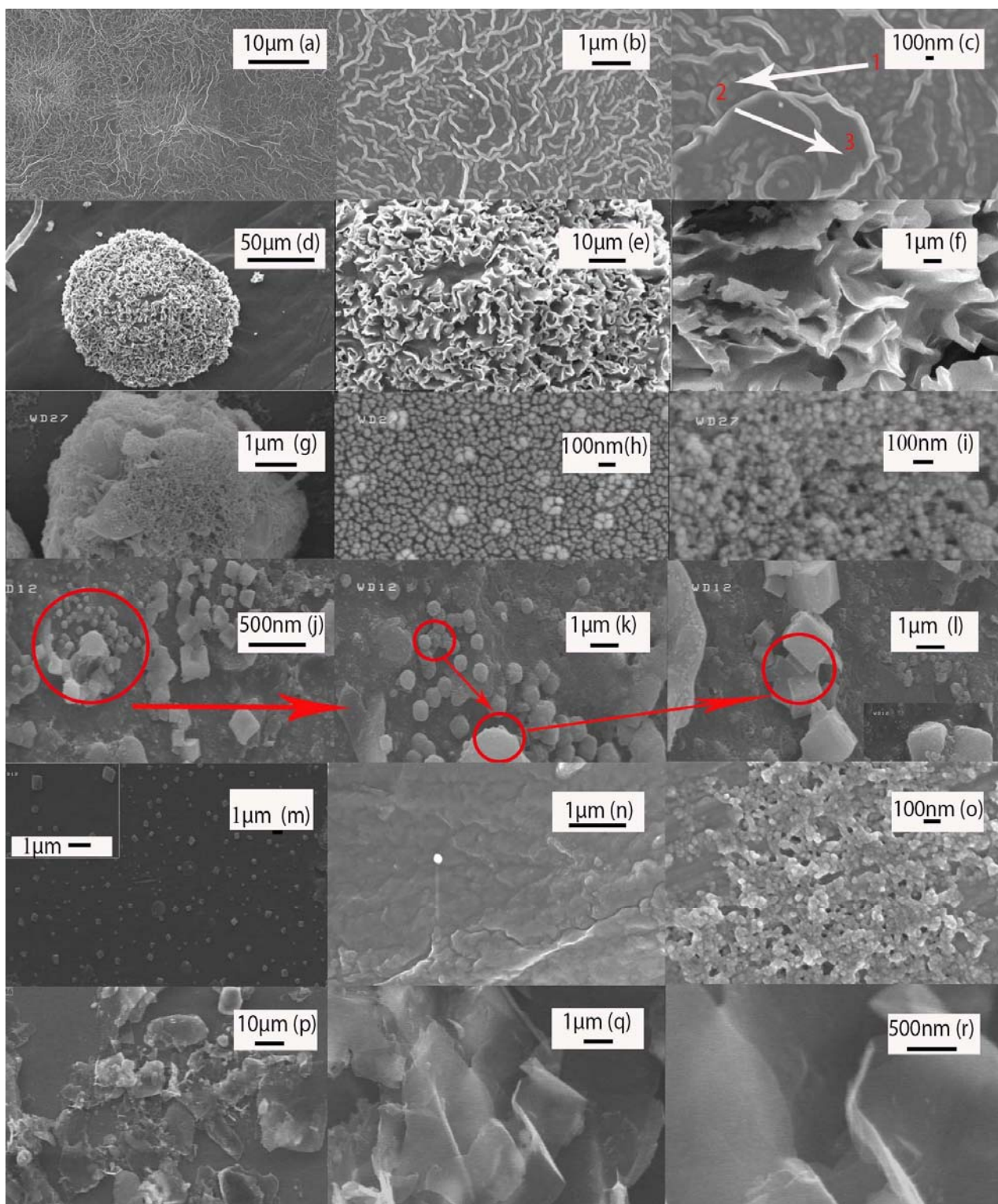


Fig. 4: SEM images of samples synthesized in: (a), (b) and (c) toluene; (d), (e) and (f) benzene; (g), (h) and (i) ethanol; (j), (k) and (l) DMA; (m), (n) and (o) hexane; and (p), (q) and (r) NMP.

The major morphological difference between the samples is the integration of the structures in the toluene- and benzene-ambient produced products with the other products. It seems aromatic structures of the solvents would prepare a favorite condition for the integration

growth of structures in the plasma plume formed by laser irradiation on top of the HOPG target [8]. The nucleation velocity is much lower than the growth velocity. However, in NMP as a cyclic amide, graphite sheets are peeled from the surface and finally

in DMA, a range of different crystal sizes are seen. These results confirm the critical role of solvent physical properties such as refractive index, viscosity, ionization energy, polarity and chemical composition on the formed plasma and also subsequent reactions in the plasma volume and on the plasma-solvent boundary which result in the formation of carbonaceous nano and microstructures.

These reactions involve the reactions of ablated species from the target with themselves, excited molecules of the solvent, and also with solvent molecules [5] which in our case composed of carbon, oxygen, hydrogen and in DMA, nitrogen too

In NMP, besides the few synthesized nanoparticles, exfoliated sheets are the major product. Shock waves produced by the adiabatic expansion of plasma plume in the liquid and its subsequent impact on the HOPG surface would be the reason of HOPG exfoliation by laser [37]. In the other five solvents, this impact is lower than the desired exfoliation threshold of the HOPG which in turns is the result of lower pressure increase in plasma plume.

### B. UV-Vis absorption

Optical absorption spectra were studied in the range of 200-900 nm. Since no remarkable feature is seen in the 400-900 nm, the initial part of the spectra in the range of 200-400 nm is investigated which is illustrated in Fig. 5. In toluene and benzene, only one peak is seen at 255 and 252 nm, respectively (Fig. (5.a-b)). In ethanol, DMA and hexane, two characteristic peaks with different maxima and widths are seen: 223 and 271 nm in ethanol (Fig. (5.c)), 237 and 267 nm in DMA (Fig. (5.d)) and also 230 and 270 nm in hexane (Fig. (5.e)). In NMP, a sharp peak at 234 nm is observed (Fig. (5.f)). Observation of peaks within 215-275 nm is the sign of carbonaceous materials. These absorption features are seen due to plasmon resonance in the free electron cloud of carbonaceous material  $\pi$  electrons. The  $\pi$  plasmon is associated with collective excitations of  $\pi$  electrons around 150-310 nm

(4-8 eV). It seems that the slight solvent remained from primary synthesis ambient and the exact graphitic structure including the shape, spatial dimension, graphitization degree, and presence of defects are the most important features which determine the overall UV-Vis spectra maxima and widths. The formation of aggregates and the agglomeration state of particles also influence the width of peaks [38]-[42].

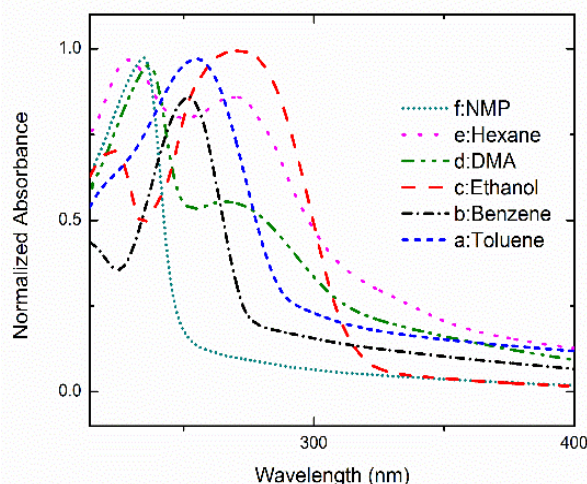


Fig. 5: UV-Vis spectra of carbon nanostructures synthesized by ablation of HOPG in different solvents.

In DMA- and hexane-ambient synthesized samples, two stronger features are visible; one at about  $233 \pm 4$  nm and a less pronounced one at around 270 nm, while in ethanol-ambient synthesized samples, the stronger peak is at 271 nm and the weaker one is somewhat seen at a shorter wavelength (223 nm). It seems that cubic and spherical graphitic particles in agglomerates and individual forms are the origin of these two typical peaks. Observation of individual peaks in the samples prepared in toluene and benzene are the result of the presence of a homogenous product with a surface plasmon resonance (SRP) of about 37 nm redshift in respect to the 217.5 nm of graphite particles. This is due to the variation in electronic structures of the nanostructured graphitic products formed in these two aromatic solvents. In NMP, graphitic nanosheets are synthesized. The observed peak at 234 nm could be assigned to either graphite

[43] or graphene oxide [44]. But the lack of shoulder in 300 nm confirms the presence of graphitic sheets.

### C. Nonlinear optical characteristics

To investigate the structure-dependent nonlinear optical properties of various carbon nanostructures, the colloidal as-synthesized samples were irradiated with a laser beam at 1.35 mJ/pulse energy in the Z-scan setup.

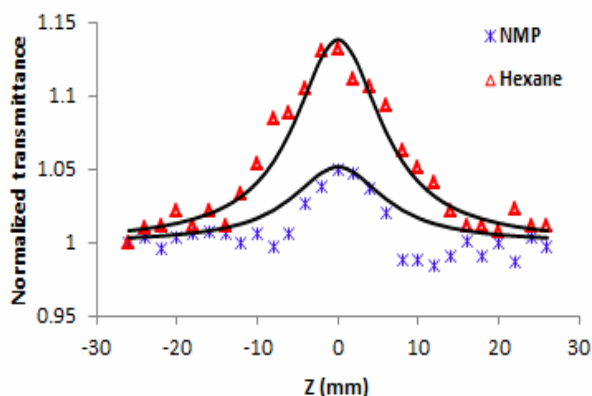


Fig. 6: The normalized open aperture Z-scan transmittance curves obtained for different structures synthesized in NMP and hexane ambient. Solid lines are numerical fits to the experimental data.

Fig. 6 represents the open-aperture (OA) Z-scan results of a 2 mm thick cell containing these structures prepared in NMP and hexane. The solid line is the theoretical fit to the experimental data according to equation (1) (see below). In NMP- and hexane-synthesized samples, a pure negative NLA, known as saturable absorption (SA) phenomenon, was measured in the OA Z-scan trace when the sample moved along the Z-axis. The difference between the Z-scan curves of these two samples is the height of the peaks that increased from 0.05 up to 0.13 values. In addition, the negative absorption of samples is strengthened in the case of the synthesized sample in hexane solvent and the response curve is broadened on the Z-axis.

As shown in Figs. (7.a-b), with the substitution of other organic solutions (DMA, toluene, benzene and ethanol) as a synthesis ambient,

the SA behaviors of produced structures are changed. Indeed, the negative absorption of samples is switched to a positive absorption, known as reverse saturable absorption (RSA) phenomenon. The nonlinear response of these samples is weak in the cauliflower-like structure synthesized in benzene. The highest nonlinearity is observed in the spiral nanowalls of the integrated structure formed in toluene ambient. To calculate the NLA coefficient ( $\beta$ ) for various carbon nanostructures, the Z-scan experimental data was theoretically fitted by normalized transmittance relation in a single OA Z-scan trace. The normalized transmittance of an OA Z-scan trace has been determined previously by Bahae *et al.* as follows [36]:

$$T(z) = \sum_{m=0}^{\infty} \frac{1}{(m+1)^{3/2}} \left[ \frac{-\beta I_0 L_{eff}}{1+(Z/Z_0)^2} \right]^m \quad (1)$$

where,  $T$  is the normalized transmittance of the open aperture Z-scan,  $I_0$  is the irradiated laser beam intensity in the focal point, and  $Z_0$  is the Rayleigh length. The  $L_{eff} = (1 - e^{-\alpha_0 L}) / \alpha_0$  is the effective length of the sample,  $L$  is the sample length (2 mm) and  $\alpha_0 = (-\ln T_0) / l$  is the sample linear absorption coefficient.  $T_0$  is the linear transmittance of the samples as illustrated in table 1 for each sample.

The calculated values of the nonlinear absorption coefficient ( $\beta$ ) for various structures are shown in table 1. The best theoretical fit is obtained by using the  $-1.1 \times 10^{-8}$  and  $-2.4 \times 10^{-8}$  ( $\text{cm W}^{-1}$ ) saturation NLA coefficients for NMP and hexane ambient, respectively. In the case of positive behavior for DMA, toluene, ethanol, and benzene ambient, values of  $3.5 \times 10^{-8}$ ,  $10.2 \times 10^{-8}$ ,  $2.5 \times 10^{-8}$ , and  $0.9 \times 10^{-8}$  ( $\text{cm W}^{-1}$ ) were obtained for positive NLA coefficients. These values are also comparable to those obtained for SWCNT and MWCNT films and graphene [35], [45], [46]. However, the value of NLA coefficient calculated for toluene-ambient suspension is higher than the calculated value measured and calculated for CNTs suspensions [47].

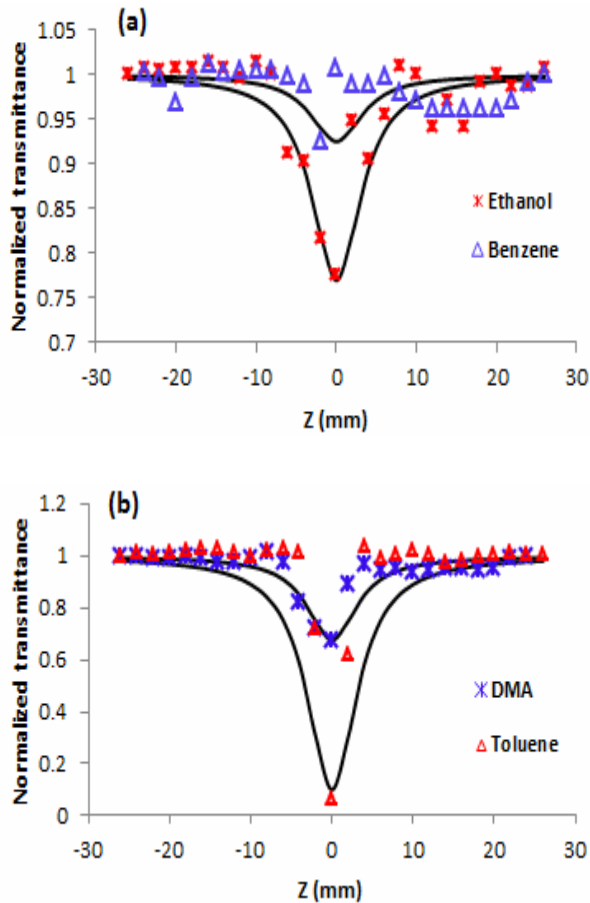


Fig. 7: The normalized open aperture Z-scan transmittance curves obtained for different structures synthesized in a) ethanol and benzene, b) DMA and toluene ambient. Solid lines are numerical fits to the experimental data.

Table 1 Values of the negative NLA coefficient ( $\beta$ ) for NMP and hexane and positive NLA coefficient ( $\beta$ ) for DMA-, benzene-, ethanol- and toluene-based synthetic products calculated from theoretical fits.

Sample	$\beta \times 10^{-8}$ (cm W <sup>-1</sup> )
Hexane	-2.4
NMP	-1.1
Benzene	0.9
Ethanol	2.5
DMA	3.5
Toluene	10.2

No exact explanations of the observed nonlinear absorption mechanism were offered in previous studies. Some speculations of the origin of the absorption involved the consideration of the electron interband transitions under the excitation of the laser. For example, the nonlinear positive absorption value of platinum NPs was attributed to the two-photon absorption mechanisms in the previous studies [48], [49]. However, the exact

mechanisms of absorption behaviors in various carbon nanostructures were not completely uncovered and further studies are needed for the definition of the processes leading to this phenomenon. Chemical bondings, particle size and morphology of the products, suspension concentration, also the laser intensity would affect the NLA values and sign [20], [48-50]. For specification of the NLA mechanisms occurred in each carbonaceous product, complicated experiments are needed.

It seems that the integrated structure produced in toluene with its unique absorption peak in 255 nm shows an outstanding NLA positive coefficient in comparison to the other products.

#### IV. CONCLUSION

Graphitic nanostructures with different morphologies were synthesized using the ablation of highly oriented pyrolytic graphite (HOPG) target in different organic solvents in an ambient condition with the inexpensive marking Q-switched neodymium: yttrium-aluminum-garnet (Nd:YAG) laser. Although, aromatic solvents of toluene and benzene stimulate the formation of integrated superstructures, laser ablation in ethanol, dimethylacetamide (DMA), and hexane result in cubic and spherical particles. However, in n-methyl-2-pyrrolidone (NMP), graphitic sheets were prepared by laser exfoliation. Apart from their morphologies, these structures showed two different nonlinear behaviors: negative and positive nonlinear absorption (saturation of absorption (SA) and reverse saturable absorption (RSA), respectively). The highest positive nonlinear optical absorption (NLA) coefficient fitted to the normalized open aperture Z-scan curves, was seen in the nanowalls prepared in toluene which is higher than carbon nanotubes (CNTs) and graphene suspensions.

## REFERENCES

- [1] R.C. Rosan, M.K. Healy, and Jr. McNary, "Spectroscopic Ultramicroanalysis with a Laser," *Science*, Vol. 142, pp. 236-237, 1963.
- [2] C. Phipps, *Laser Ablation and its Applications*, USA: Springer, 2007.
- [3] A. Kabashin. "Laser Ablation-Based Methods for Nanostructuring of Materials," *Laser Phys.* Vol. 19, pp. 1136-1141, 2009.
- [4] P. Liu, H. Cui, C.X. Wang, and G.W. Yang. "From Nanocrystal Synthesis to Functional Nanostructure Fabrication: Laser Ablation in Liquid," *Phys. Chem. Chem. Phys.* Vol. 12, pp. 3942-3952, 2010.
- [5] G. Yang, ed. *Laser Ablation in Liquids: Principles and Applications in the Preparation of Nanomaterials*, Singapore: Pan Stanford Publishing Pte. Ltd. 2012.
- [6] N.G. Semaltianos. "Nanoparticles by Laser Ablation," *Crit. Rev. Solid State*, Vol. 35, pp. 105-124, 2010.
- [7] S.E. Black, ed. *Laser Ablation in Liquids : Effects and Applications, Lasers and Electro-Optics Research and Technology*, Nova Science Publishers Inc. New York, 2011.
- [8] G.W. Yang. "Laser Ablation in Liquids: Applications in the Synthesis of Nanocrystals," *Prog. Mater. Sci.* Vol. 52, pp. 648-698, 2007.
- [9] S.E. Johnson, M.N.R. Ashfold, M.P. Knapper, R.J. Lade, K.N. Rosser, N.A. Fox, and W.N. Wang. "Production and Characterisation of Amorphous Diamond Films Produced by Pulsed Laser Ablation of Graphite," *Diamond Relat. Mater.* Vol. 6, pp. 569-673, 1997.
- [10] J.B. Wang, C.Y. Zhang, X.L. Zhong, and G.W. Yang. "Cubic and Hexagonal Structures of Diamond Nanocrystals Formed Upon Pulsed Laser Induced Liquid-Solid Interfacial Reaction," *Chem. Phys. Lett.* Vol. 361, pp. 86-90, 2002.
- [11] E. Munoz, W.K. Maser, A.M. Benito, M.T. Martinez, G.F. de la Fuente, A. Righi, E. Anglaret, and J.L. Sauvajol. "The Influence of the Target Composition in the Structural Characteristics of Single-Walled Carbon Nanotubes Produced by Laser Ablation," *Synth. Met.* Vol. 121, pp. 1193-1194, 2001.
- [12] H. Tabata, M. Fujii, and S. Hayashi. "Synthesis of Polyynes by Laser Ablation of Diamond Nanoparticles Suspended in Solution," *Europ. Phys. J. D*, Vol. 34, pp. 223-225, 2005.
- [13] T. F.Kuo, C.C. Chi, and I.N. Lin. "Synthesis of Carbon Nanotubes by Laser Ablation of Graphites at Room Temperature," *Japan. J. Appl. Phys. Part 1-Regular Papers Short Notes Review Papers*, Vol. 40, pp. 7147-7150, 2001.
- [14] A. Kruusing. *Handbook of Liquids-Assisted Laser Processing*, Elsevier, Amsterdam, 2008.
- [15] L. Berthe, R. Fabbro, P. Peyre, L. TOLLIER, and E. Bartnicki. "Shock Waves from a Water-Confined Laser-Generated Plasma," *J. Appl. Phys.* Vol. 82, pp. 2826-2832, 1997.
- [16] L. Yang, P.W. May, L. Yin, J.A. Smith, and K.N. Rosser. "Growth of Diamond Nanocrystals by Pulsed Laser Ablation of Graphite in Liquid," *Diamond and Related Mater.* Vol. 16, pp. 725-729, 2007.
- [17] H. Hidai and H. Tokura. "Diamond Like Carbon Particle Synthesis in the Water by Laser Irradiation," *J. the Japan. Soc. Precision Eng.* Vol. 68, pp. 1072-1076, 2002.
- [18] G.W. Yang and J.B. Wang. "Carbon Nitride Nanocrystals Having Cubic Structure Using Pulsed Laser Induced Liquid-Solid Interfacial Reaction," *Appl. Phys. A: Materials Science and Processing*, Vol. 71, pp. 343-344, 2000.
- [19] G. Compagnini, V. Mita, R.S. Catalotti, L. D'Urso, and O. Puglisi. "Short Polyene Chains Produced by Pulsed Laser Ablation of Graphite in Water," *Carbon*, Vol. 45, pp. 2456-2458, 2007.
- [20] G.X. Chen, M.H. Hong, T.C. Chong, H.I. Elim, G.H. Ma, and W. Ji. "Preparation of Carbon Nanoparticles with Strong Optical Limiting Properties by Laser Ablation in Water," *J. Appl. Phys.* Vol. 95, pp. 1455-1459, 2004.
- [21] L. Yang, P. May, L. Yin, J. Smith, and K. Rosser. "Ultra Fine Carbon Nitride Nanocrystals Synthesized by Laser Ablation in Liquid Solution," *J. Nanopart. Res.* Vol. 9, pp. 1181-1185, 2007.
- [22] S.I. Kitazawa, H. Abe, and S. Yamamoto. "Formation of Nanostructured Solid-State Carbon Particles by Laser Ablation of

- Graphite in Isopropyl Alcohol,” *J. Phys. Chem. Solids*, Vol. 66, pp. 555-559, 2005.
- [23] M. Tsuji, S. Kuboyama S. Kuboyama, S.-H. Yoon, Y. Korai, T. Tsujimoto, K. Kubo, and A. Mori, “Formation of Hydrogen-Capped Polyynes by Laser Ablation of Graphite Particles Suspended in Solution,” *Chem. Phys. Lett.* Vol. 355, pp. 101-108, 2002.
- [24] S.B. Ogale, A.P. Malshe, S.M. Kanetkar, and S.T. Kshirsagar. “Formation of Diamond Particulates by Pulsed Ruby Laser Irradiation of Graphite Immersed in Benzene,” *Solid State Commun.* Vol. 84, pp. 371-373, 1992.
- [25] C.X. Wang, P. Liu, H. Cui, and G.W. Yang. “Nucleation and Growth Kinetics of Nanocrystals Formed Upon Pulsed-Laser Ablation in Liquid,” *Appl. Phys. Lett.* Vol. 87, pp. 1-3, 2005.
- [26] M. Shusser. “Kinetic Theory Analysis of Laser Ablation of Carbon: Applicability of One-Dimensional Models,” *J. Appl. Phys.* Vol. 101, pp. 036103 (1-6), 2007.
- [27] Q.X. Liu, C.X. Wang, and G.W. Yang. “Nucleation Thermodynamics of Cubic Boron Nitride in Pulsed-Laser Ablation in Liquid,” *Phys. Rev. B: Condens. Matter*, Vol. 71, pp. 155422 (1-6), 2005.
- [28] A. Mangione, L. Torrisi, A. Picciotto, F. Caridi, D. Margarone, E. Fazio, A. La Mantia, and G. Di Marco. “Carbon Nanocrystals Produced by Pulsed Laser Ablation of Carbon,” *Radiat. Eff. Defects Solids*, Vol. 160, pp. 655-562, 2005.
- [29] K.C. Chin, A. Gohel, W.Z. Chen, H.I. Elim, W. Ji, G.L. Chong, C.H. Sow, and A.T.S. Wee. “Gold and Silver Coated Carbon Nanotubes: An Improved Broad-Band Optical Limiter,” *Chem. Phys. Lett.* Vol. 409, pp. 85-88, 2005.
- [30] S.R. Mishra, H.S. Rawat, S.C. Mehendale, K. C. Rustagi, A.K. Sood, R. Bandyopadhyay, A. Govindaraj, and C.N. R. Rao. “Optical Limiting in Single-Walled Carbon Nanotube Suspensions,” *Chem. Phys. Lett.* Vol. 317, pp. 510-514, 2000.
- [31] L. Vivien, E. Anglaret, D. Riehl, F. Bacou, C. Journet, C. Goze, M. Andrieux, M. Brunet, F. Lafonta, P. Bernier, and F. Hache. “Single-Wall Carbon Nanotubes for Optical Limiting,” *Chem. Phys. Lett.* Vol. 307, pp. 317-319, 1999.
- [32] A.V. Ellis, K. Vijayamohanam, R. Goswami, N. Chakrapani, L.S. Ramanathan, P.M. Ajayan, and G. Ramanath. “Hydrophobic Anchoring of Monolayer-Protected Gold Nanoclusters to Carbon Nanotubes,” *Nano Lett.* Vol. 3, pp. 279-282, 2003.
- [33] J. Wang, M. Feng, and H. Zhan. “Preparation, Characterization, and Nonlinear Optical Properties of Graphene Oxide-Carboxymethyl Cellulose Composite Films,” *Opt. Laser Technol.*, Vol. 57, pp. 84-89, 2014.
- [34] B.S. Kalanoor, P.B. Bisht, S. Akbar Ali, T.T. Baby, and S. Ramaprabhu. “Optical Nonlinearity of Silver-Decorated Graphene,” *J. Opt. Soc. Amer. B*, Vol. 29, pp. 669-675, 2012.
- [35] Z.B. Liu, X.L. Zhang, X.Q. Yan, Y.S. Chen, and J.G. Tian. “Nonlinear Optical Properties of Graphene-Based Materials,” *Chin. Sci. Bull.* Vol. 57, pp. 2971-2982, 2012.
- [36] M. Sheik-Bahae, A.A. Said, T.H. Wei, D.J. Hagan, and E.W. Van Stryland. “Sensitive Measurement of Optical Nonlinearities Using a Single Beam,” *IEEE J. Quantum Electron.* Vol. 26, pp. 760-769, 1990.
- [37] H. Ghanabari, *Synthesis of graphene nanosheets by laser ablation and applying on glass*, Ph.D. thesis, Dept. Eng., Tarbiat Modares University, Tehran, Iran, 2014.
- [38] Y. Kimura. “Production and Structural Characterization of Carbon Soot with Narrow Uv Absorption Feature,” *Carbon*, Vol. 42, pp. 33-38, 2004.
- [39] G.A. Rance, D.H. Marsh, R.J. Nicholas, and A.N. Khlobystov. “Uv-Vis Absorption Spectroscopy of Carbon Nanotubes: Relationship between the  $\Pi$ -Electron plasmon and Nanotube Diameter,” *Chem. Phys. Lett.* Vol. 493, pp. 19-23, 2010.
- [40] S. Tomita, S. Hayashi, Y. Tsukuda, and M. Fujii. “Ultraviolet-Visible Absorption Spectroscopy of Carbon Onions,” *Phys. Solid State*, Vol. 44, pp. 450-453, 2002.
- [41] P. Liu, Y.L. Cao, C.X. Wang, X.Y. Chen, and G.W. Yang. “Micro- and Nanocubes of Carbon with C8-Like and Blue Luminescence,” *Nano Lett.* Vol. 8, pp. 2570-2575, 2008.
- [42] I. Lamas-Jansa, C. Jager, H. Mutschke, and T. Henning. “Far-Ultraviolet to near-Infrared

Optical Properties of Carbon Nanoparticles Produced by Pulsed-Laser Pyrolysis of Hydrocarbons and Their Relation with Structural Variations,” *Carbon*, Vol. 45, pp. 1542-1557, 2007.

- [43] N. Liu, F. Luo, H. Wu, Y. Liu, C. Zhang, and J. Chen. “One-Step Ionic-Liquid-Assisted Electrochemical Synthesis of Ionic-Liquid-Functionalized Graphene Sheets Directly from Graphite,” *Adv. Funct. Mater.*, Vol. 18, pp. 1518-1525, 2008.
- [44] F. Li, Y. Bao, J. Chai, Q. Zhang, D. Han, and L. Niu. “Synthesis and Application of Widely Soluble Graphene Sheets,” *Langmuir*, Vol. 26, pp. 12314-12320, 2010.
- [45] J. Wang, K.-S. Liao, D. Früchtl, Y. Tian, A. Gilchrist, N.J. Alley, E. Andreoli, B. Aitchison, A.G. Nasibulin, H.J. Byrne, E.I. Kauppinen, L. Zhang, W.J. Blau, and S.A. Curran. “Nonlinear Optical Properties of Carbon Nanotube Hybrids in Polymer Dispersions,” *Mater. Chem. Phys.* Vol. 133, pp. 992-997, 2012.
- [46] H.I. Elim, W. Ji, G.H. Ma, K.Y. Lim, C.H. Sow, and C.H. Huan. “Ultrafast Absorptive and Refractive Nonlinearities in Multiwalled Carbon Nanotube Films,” *Appl. Phys. Lett.* Vol. 85, pp. 1799-1801, 2004.
- [47] J. Wang, Y. Chen, and W.J. Blau. “Carbon Nanotubes and Nanotube Composites for Nonlinear Optical Devices,” *J. Mater. Chem.* Vol. 19, pp. 7425-7443, 2009.
- [48] R.A. Ganeev, R.I. Tugushev, and T. Usmanov. “Application of the Nonlinear Optical Properties of Platinum Nanoparticles for the Mode Locking of Nd:Glass Laser,” *Appl. Phys. B*, Vol. 94, pp. 647-651, 2009.
- [49] A. Chehrghani, and M.J. Torkamany. “Nonlinear Optical Properties of Laser Synthesized Pt Nanoparticles: Saturable and reverse Saturable Absorption,” *Laser Phys.* Vol. 24, pp. 015901 (1-7), 2014.
- [50] Y. Hongzhi. *Saturable Absorption and Two-Photon Absorption in Graphene*, Ph.D. thesis, Shandong University, Shandong, China, 2012.



**Hajar Ghanbari** was born in Tehran, in 1982. She received her BSc and MSc from Iran University of Science and Technology in 2003 and 2006, respectively in Materials Engineering, Ceramics. She received her Ph. D. in 2014 in Ceramics from Tarbiat Modares University, Tehran, Iran. She has worked on nanoparticles and carbon nanomaterials synthesis and characterization. She has 14 journal and conference articles.



**Rasoul Sarraf-Mamoory** received his BSc and MSc from Tehran University, Tehran, Iran in 1984 and 1986, respectively in Metallurgy and his Ph.D. in Powder Metallurgy in 1992 from McGill University, Canada. He has continued his academic career in Tarbiat Modares University, Tehran, Iran as an associate professor. He has more than 150 journal and conference papers and supervised more than 50 students.



**Jamshid Sabbaghzadeh** received his BSc in Physics from Sharif University. He has continued his studies in Texas State University on USA and received his MSc in Atomic & Molecular Physics in 1990 and his Ph. D. in Quantum Electronics in 1995 from this university. He has taught different courses in Tehran University, Shahid Beheshti University and Azad University and also supervised more than 50 graduate students. He is a full professor now and the founder of Iranian National Center for Laser Science and Technology.



**Ali Chehrghani** was born in Saveh in 1983. He received his BSc in Bu-Ali Sina University in 2005 & MSc in Iran University of Science & Technology in 2007 both in Atomic and Molecular Physics. He works in Iranian National Center for Laser Science &

Technology. He has 15 conference and journal papers. His current research is the investigation in the application of lasers in material processing and nonlinear optical properties of nanomaterials.



**Rasoul Malekfar** received his BSc in Physics in 1980 from Pars College, Tehran, I.R. Iran, MSc in theoretical Physics in 1984 from University of Kent at Canterbury, U.K. and his Ph. D. in experimental Physics, laser Raman spectroscopy, from King's College, University of London in 1989. He is currently engaged as a full professor of Physics in Atomic and Molecular group, Physics Department, Tarbiat Modares University, Tehran, Iran.